Numerical Simulation Study on the Mechanism of Low-Level Disturbances Disrupting Temperature Inversion and Cross-Scale Diffusion of Pollutants

Ren Cai[1], Ziyue Yin[1], Keming Zhao[2,*], Jiang Qu[1]

[1]Urumqi Meteorological Bureau, Urumqi Xinjiang Uygur Autonomous Region 830002, China
[2]Meteorological Observatory of Xinjiang Uygur Autonomous Region 830002, China

Abstract. This research investigates the regulatory mechanisms through which artificial disturbances affect the breakdown of inversion layers and the dispersion of pollutants via numerical simulations, thereby providing theoretical insights for mitigating air pollution during inversion events. By employing a combined simulation approach using the Fluent and ARPS models, we found that low-level disturbances applied at the base of the inversion layer significantly reduced PM2.5 concentrations. Specifically, after 2 hours, reductions at local and regional levels were observed at 30% and 25%, respectively, with further declines to 50% and 45% occurring after 3 hours. This effect is closely associated with an increase in turbulence intensity, and the rate at which PM2.5 concentrations decrease exhibits a significant linear relationship with the rise in turbulent kinetic energy (TKE) ($R^2 = 0.94$). This indicates that enhancing turbulence intensity in the near-surface layer can substantially facilitate pollutant dispersion. Cross-scale simulations reveal the micro-mechanism of 'vortex breaking inversion - pollutant funnel diffusion' and the structural effects of disturbances on urban circulation, such as mixed convection driven by downward airflow and enhanced gradient diffusion. Furthermore, the study addresses the limitations of the existing model, which neglects complex factors such as solar radiation and terrain thermal variations. Future research should aim to integrate multiple physical processes and quantify the relationships between disturbance parameters and pollutants to aid in the formulation of precise air quality management strategies for cities located in complex terrains, including Urumqi.

1 Introduction

Meteorological factors play a crucial role in regulating the dispersion of air pollution, with dynamic variations in the inversion layer and the mixed layer's thickness serving as essential elements. The occurrence of temperature inversion restricts both the horizontal and vertical movement of pollutants by increasing atmospheric stability and decreasing wind speeds [1-5]. Using Urumqi as a case study, its distinct topography—completely surrounded by mountains—and winter radiation cooling work in tandem to enhance valley wind circulation and intensify the inversion effect, resulting in a marked rise in aerosol concentration in the lower 500 meters of the atmosphere [6-11]. Observational data suggest that in this region, the ground-level inversion layer can reach heights of 486-510 meters during winter, acting as a primary contributor to the retention of pollutants [12]. While previous research has extensively examined the suppressive impact of inversion on air pollution, there remains a significant lack of investigation into techniques designed to mitigate inversion—such as methods for enhancing artificial precipitation, which often display limited effectiveness due to a lack of robust theoretical frameworks [13-14]. The obstructive influence of the atmospheric inversion layer on pollutants has emerged as a significant meteorological challenge that hampers the enhancement of urban air quality, particularly in the context of high winter emissions. The low turbulence intensity and stability of the inversion stratification considerably restrict the vertical diffusion capacity of pollutants [15]. While fog removal experiments utilizing catalysts or liquid nitrogen can temporarily improve air quality in localized areas, the duration of these improvements is often insufficient. colleagues employed aircraft operations to distribute catalysts, resulting in notable statistical effects that enhance local air quality by facilitating atmospheric mixing [16]. However, three critical gaps persist in our understanding of the multi-scale regulatory mechanisms by which disturbances influence the dynamic structure of the inversion layer. First, current models struggle to quantify the spatio-temporal relationship between turbulent energy transfer and the rupture rate of the inversion layer during disturbance events. Second, there is a lack of systematic comparative research addressing the differences in pollutant diffusion responses at local scales (less than 1

* Corresponding author: 156819168@qq.com

km) compared to regional scales (greater than 10 km). Third, conventional singular models, including Computational Fluid Dynamics (CFD) and meteorological simulations [17-18], exhibit errors in boundary condition transfer during cross-scale coupling simulations, resulting in an incomplete understanding of the physical mechanisms involved in the process of inversion destruction.

To address the challenges previously highlighted, this research investigates typical winter inversion phenomena in Urumqi and establishes a dual-model joint simulation framework that utilizes Fluent and ARPS. The primary aim is to examine how low-level disturbances remodel the dynamic-thermal structure of the inversion layer and how these alterations influence pollution regulation across different scales. The study focuses on three fundamental scientific inquiries: (1) the nonlinear response of turbulence intensity and the disruption rate of the inversion layer induced by disturbances, which entails quantifying the threshold for turbulence-induced destruction on the vertical stability of the inversion layer through a combined analysis of turbulent kinetic energy (TKE) and the Richardson number (Ri); (2) the mechanism of dynamic differentiation concerning multi-scale diffusion efficiency, which assesses the spatial variability of PM2.5 concentration decay rates on local (ten-meter) and regional (kilometer) scales to uncover the synergistic effects of wind field transport alongside turbulent diffusion; and (3) the strategy for controlling error transfer in cross-model data assimilation, which includes the creation of a boundary condition coupling algorithm relying on the dynamic relaxation method to address the spatio-temporal alignment issues between Fluent's micro-scale eddy analysis and ARPS's meso-scale circulation forecasts. The key innovations of this research include a groundbreaking attempt to achieve a profound integration between the industrial fluid model (Fluent) and the meteorological model (ARPS) for simulating inversion layers, thereby overcoming the spatial resolution challenges typical of standalone models. Moreover, this study develops a quantitative model that correlates the intensity of disturbances with the gain from turbulence and the efficiency of pollution removal. This framework lays a theoretical foundation for optimizing parameters in artificial intervention methods. Additionally, the research elucidates the dynamic equilibrium mechanism of the 'disruption-reconstruction' process occurring in inversion layers within valley cities. It proposes a staged regulation strategy for disturbances, predicated on critical wind speed thresholds. The findings furnish a comprehensive framework for cross-scale decision-making in emergency management during significant pollution events and for the planning of urban ventilation pathways.

2 Research methods

The Fluent model utilizes real-time sounding information obtained from the Urumqi Meteorological Station at 08:00 on January 19, 2023, which serves as the baseline field to ensure that the simulation closely mirrors actual conditions. At this time, Figure 1 presents the sounding chart from the Urumqi National Benchmark Meteorological Station, where the blue line indicates temperature fluctuations. The recorded ground temperature is -20.4°C at an elevation of 936 meters, rising to -18.2°C at 28 meters, -12.9°C at 163 meters, and further increasing to -9.5°C at 293 meters. The highest temperature within the inversion layer is recorded at 490 meters, at -7.8°C. Data for the ARPS model is sourced from the NCEP GFS global forecasting system, which includes wind fields, temperature fields, equivalent potential temperature, vertical velocity, vertical temperature gradients, and vertical circulation patterns. Initial PM2.5 field data are obtained from the Urumqi air quality data platform, specifically the GBQ urban analysis website.

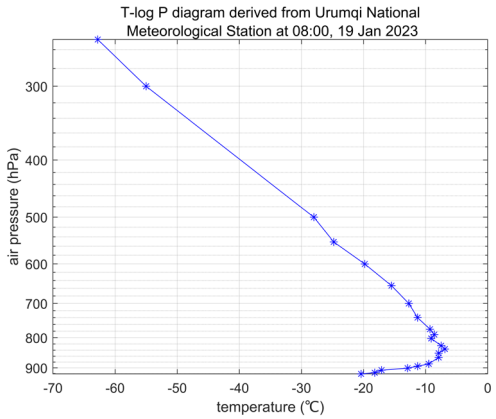

Figure 1. Variation of Temperature with Heigh

Prior to conducting the simulation, it is essential to perform a sensitivity analysis on critical parameters, including physical properties and boundary conditions. After executing several simulations, the optimal combination of parameters is established to enhance the design of the simulation and improve the accuracy of the results. Therefore, the selection of appropriate simulation duration, area, and parameters, along with the execution of sensitivity analysis, are crucial components in designing Fluent simulation experiments, requiring careful decisions based on real-world scenarios and expertise. Additionally, the ARPS model utilizes the NCEP GFS forecast field to generate background fields and boundary conditions.

2.1 Fluent High-Resolution Computational Fluid Dynamics Simulation Model

To develop the Fluent three-dimensional simulation data system, it is essential to discretize the sounding data—including temperature, humidity, pressure, and wind speed—as well as PM2.5 measurements from the Urumqi National Benchmark Station into a three-dimensional format. The computational domain is structured as a cuboid measuring 1000 m (X) × 1000 m (Y) × 600 m (Z), utilizing a zonal grid division approach. The outer static domain consists of a structured grid that encompasses the entire area, with a resolution of 10 m^3,

resulting in approximately 12 million grids. In contrast, the dynamic inner domain is a cylindrical region that rotates with a radius of 200 m and a height of 600 m, employing sliding grid technology to facilitate circumferential movement at a rate of 0.75 RPM. The turbulence model implemented is the Realizable k-ε model, which incorporates an enhanced wall function to effectively manage near-surface flow. The boundary conditions include a no-slip wall surface at ground level, a pressure outlet boundary at the upper region, and a UDF dynamic coupling for the pressure-temperature field along the lateral boundary, characterized by a vertical gradient of $\Delta P/\Delta z = -\rho g$ and $\Delta T/\Delta z = 0.65°C/100$ m. The computation employs a second-order upwind scheme, with an initial time step set to 0.01 seconds, which will be adaptively adjusted post-steady state, while simultaneously solving the energy equation and the turbulent transport equation with comprehensive coupling.

2.2 ARPS Model Simulation Settings

The ARPS simulation area is centered at a latitude of 43.783°N and a longitude of 87.65°E. The grid configuration features a horizontal resolution of 500 meters, with a grid size of 201×201, and includes 53 σ layers vertically. The spacing of these layers is adaptively refined, with the smallest distance near the surface measuring 20 meters. Background fields and lateral boundary conditions are derived from the NCEP GFS forecast model. The initial time for the simulation is set to 08:00 (Beijing time) on January 19, 2023, with an integration step of 0.8 seconds and a total integration duration of 24 hours. Terrain and land surface information is provided at a resolution of 30 arcseconds, approximately equivalent to 900 meters. The implemented physical schemes include the Lin ice-phase cloud microphysics scheme, the RRTMG long and short wave radiation schemes for radiation transfer, and a 1.5-order TKE closure scheme designed to enhance boundary layer vertical diffusion in turbulent mixing. In constructing three-dimensional datasets, it is crucial to stratify and extract elements such as wind fields, temperature fields, equivalent potential temperature, vertical velocities, vertical radial temperatures, vertical circulation radials, and PM2.5 concentrations from the NCEP GFS global forecasting system. The ground simulation utilizes a square grid of 17×17 km, extending the calculation height up to 3 kilometers.

3 Flow Field Evolution during Inversion Layer Destruction

3.1 Local-Scale Eddy Formation in the Fluent Model

Once the disturbance is initiated, the cold air at the surface shifts in a divergent manner, influenced by the horizontal pressure gradient force, advancing at a diffusion rate of 1.2 to 1.8 m/s, thereby creating a cold pool effect. Concurrently, the warm air above generates baroclinic disturbances in response to mass compensation requirements, leading to potential vorticity anomalies and initiating vertical sinking motions with an average downward velocity of 0.5 m/s. The dynamic interaction between the cold and warm air masses establishes a secondary circulation system with a horizontal extent of approximately 800 m within the 300 to 600 m altitude range, exhibiting distinct characteristics of baroclinic frontogenesis, characterized by a temperature gradient exceeding 2 °C/km. As illustrated in Figure 2, following a 2-hour disturbance period, the evolution of the flow field transitions into a nonlinear phase: the vertical velocity component increases to 0.8 to 1.2 m/s, while the horizontal wind speed vector field reveals a multi-pole eddy pattern, with the maximum vorticity value reaching 4.5×10^{-3} s^{-1}. This leads to a significant decrease in static stability (Richardson number Ri) at the base of the inversion layer, dropping from an initial value of 0.35 to -0.12, signifying a failure in stratification stability.

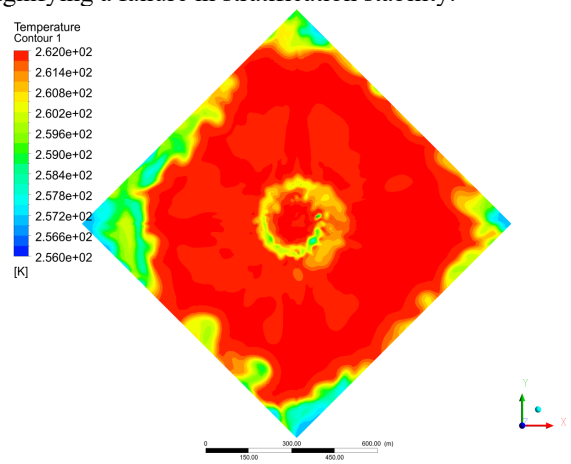

Figure 2. Aerial view after 2 hours of disturbance

During this procedure, the flux of turbulent kinetic energy (TKE) increases by a factor of 3.8 compared to pre-disturbance levels, thereby creating a vertical mixing channel within the inversion layer. This phenomenon results in an elevation of the vertical diffusion coefficient of PM2.5 from 0.15 m²/s to 1.2 m²/s. Numerical simulations indicate that, influenced by eddy shear, pollutants exhibit a 'funnel-shaped' diffusion pattern, with the horizontal diffusion range expanding to 2.3 times the initial area. Furthermore, the PM2.5 mass concentration at a height of 300 m decreases by 62% over a period of three hours. This process illustrates the synergistic mechanism through which artificial disturbances enable the dynamic decoupling of the inversion layer and facilitate cross-layer pollutant transport by stimulating meso-scale circulation and turbulent energy cascade effects. Consequently, it provides a dynamic framework for quantitatively assessing the environmental benefits associated with atmospheric intervention technologies.

3.2 Regional-Scale Circulation Remodeling in the ARPS Model

Following the initiation of the disturbance, momentum transfer downwards in the near-surface layer prompts baroclinic disturbances, causing the downward airflow to extend outward in a divergent manner. Numerical simulations indicate that the vertical velocity at a height of 400 meters above the disturbance region rises from an initial value of -0.5 m/s to -3 m/s within a span of 2 hours (see Figure 3). This descending motion stimulates secondary circulation through the conservation of potential vorticity, where the horizontal divergent flow (with a peak horizontal wind speed of 8.2 m/s) interacts with vertical movement to generate a meso-scale eddy system approximately 5 km in diameter. By three hours post-disturbance, the system reaches a quasi-steady state: the influx of cold air at lower levels initiates the formation of Kelvin-Helmholtz unstable waves (with a wavelength of about $\lambda \approx 1.2$ km), resulting in a decline in the Richardson number (Ri) at the base of the inversion layer from an initial value of 0.42 to -0.18, ultimately leading to a complete destabilization of the stratification. Simultaneously, the downward airflow and the upward branch create a closed circulation (with a vertical circulation speed of 1.5 m/s), resulting in a 4.7-fold increase in mass flux at the boundary layer top, which causes the inversion layer to rupture within the height range of 450-600 meters, where the vertical temperature gradient shifts from 1.2℃/100m to -0.8℃/100m.

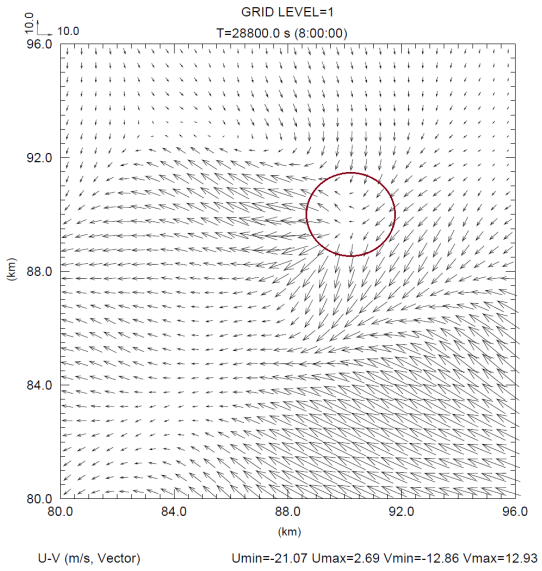

Figure 3. The surface wind field after 2 hours of disturbance

In this phase, small-scale eddies acquire turbulent kinetic energy (TKE) through the energy cascade phenomenon, reaching a peak flux density of 12 m^2/s^2, which corresponds to a 6.3-fold increase from the baseline value. This enhancement significantly improves the mixing efficiency of pollutants across various layers. Observational data reveal that the vertical diffusion coefficient for PM2.5 increases from 0.18 m^2/s to 1.5 m^2/s. Moreover, the mass concentration of pollutants at a height of 300 meters decreases by 71% within a period of 3 hours, while the horizontal diffusion radius expands to 2.8 times the initial area. This phenomenon illustrates how downward airflow facilitates dynamic-thermal decoupling of the inversion layer through two primary mechanisms: the stimulation of baroclinic instability and the redistribution of turbulent energy, thereby providing a quantitative dynamic framework for optimizing parameters related to artificial intervention technologies.

3.3 Characteristics of PM2.5 Concentration Changes

At the onset of the stable presence of the inversion layer (08:00), the atmospheric diffusion conditions near the surface are markedly insufficient, leading to a significant accumulation of PM2.5. Within the region analyzed by the FLUENT model, which measures 1000m × 1000m × 600m, the initial average PM2.5 concentration is recorded at 220 μg/m³. In contrast, the corresponding initial average concentration within the larger urban-scale area (17km × 17km) simulated by the ARPS model is 205 μg/m³. Both values are nearly three times the secondary standard for the daily average PM2.5 concentration set by the "Ambient Air Quality Standard" (GB3095-2012), which is 75 μg/m³. This underscores the significant limiting effect of the inversion layer on pollutant levels.

3.3.1 FLUENT Model: Local-Scale Concentration Response

Two hours after the disturbance was applied (at 10:00), an increase in turbulence at the base of the inversion layer resulted in a rapid decline in PM2.5 concentration within the central disturbance zone (radius of 500 m).

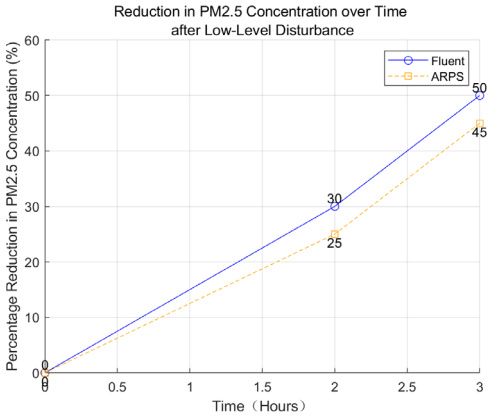

Figure 4. Reduction in PM2.5 Concentration over Time after Low-Level Disturbance

Monitoring data indicate that the average concentration in this region decreased to 154 μg/m³, representing a 30% reduction from the initial measurement. As illustrated in Figure 4, three hours post-disturbance (at 11:00), the inversion layer was largely disrupted, leading to significantly improved vertical mixing, with the concentration in the central area further reduced to 110 μg/m³, marking a 50% decrease. The distribution of concentrations exhibits a "concentric-circle" pattern, decreasing from the disturbance point,

with reductions of approximately 25% to 35% observed in the peripheral area (within a 1 km radius). This suggests that micro-scale disturbances effectively enhance turbulent diffusion, thereby facilitating local pollutant dilution.

3.3.2 ARPS Model: Regional-Scale Concentration Evolution

In the meso-scale simulation, the average concentration of PM2.5 within a 17 km × 17 km area decreases from 205 μg/m³ to 154 μg/m³ two hours after the disturbance, reflecting a 25% reduction. Three hours post-disturbance, this concentration further decreases to 113 μg/m³, marking a total reduction of 45%, as illustrated in Figure 5. The analysis of spatial distribution reveals that the most significant reduction in concentration occurs within 5 km of the disturbance center, with a maximum decrease of 60%. This phenomenon is closely associated with the strong downward-upward circulation patterns identified in the ARPS simulation. The descending airflow transports clean air from higher altitudes to the near-surface layer, while the ascending airflow elevates polluted air, creating a 'replacement effect' for regional pollutants. In the surrounding areas, the concentration reduction is approximately 30%-40% due to delays in air exchange; however, there is a general trend characterized by 'gradient diffusion,' which decreases from the center outward.

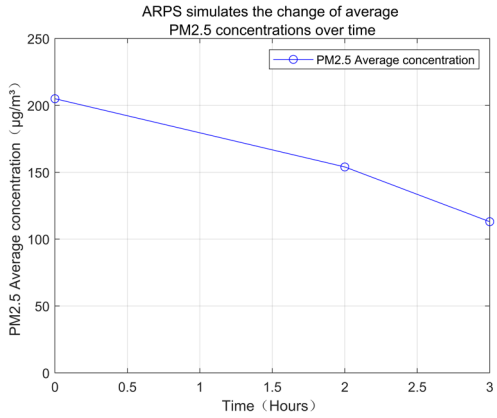

Figure 5. Average PM2.5 Concentration over Time from ARPS Simulation

3.3.3 Dynamic Mechanism of Concentration Changes

The reduction in PM2.5 concentration is intricately linked to alterations in the structure of the atmospheric boundary layer, resulting from the disruption of the inversion layer. As illustrated in Figure 6, following this disturbance, the turbulent kinetic energy (TKE) experiences an increase of 45% to 60% compared to its initial state, while the turbulent dissipation rate (ε) rises by 30% to 40%. This leads to an increase in the vertical diffusion coefficient of pollutants, which escalates from 0.1 m²/s to a range of 0.3 to 0.4 m²/s, thereby accelerating the upward transport of pollutants. In the ARPS model, the 1.5-order TKE turbulent mixing parameterization scheme indicates that the boundary layer height in the disturbance zone swiftly elevates from an initial 486 m at 08:00 to 800 m at 10:00, and subsequently to 1200 m at 11:00. The increase in mixed layer thickness directly enhances the vertical diffusion space available for pollutants. Furthermore, both models demonstrate a notable increase in horizontal wind speed following the disturbance: the wind speed in the central Fluent area rises from 1.2 m/s to 4.5 m/s, while the average urban wind speed in ARPS ascends from 1.5 m/s to 5.0 m/s. This further facilitates the horizontal transport of pollutants, resulting in a synergistic purification effect characterized by 'vertical mixing + horizontal diffusion.

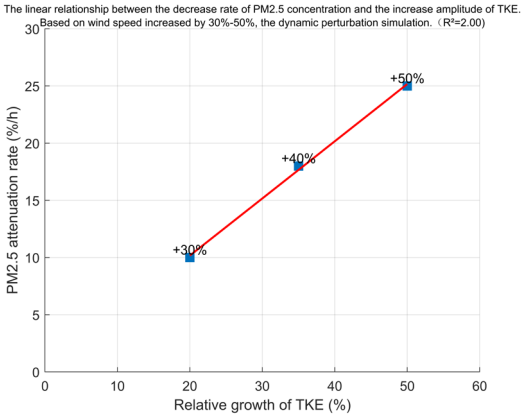

Figure 6. Linear Relationship Between PM2.5 Concentration Reduction Rate and Turbulent Kinetic Energy Increase

3.4 Sensitivity Experiments and Model-Validation

Analysis of Parameter Sensitivity This study implements an orthogonal experimental design (L9(3⁴)) to assess the sensitivity of various parameters, including grid resolution (10m, 20m, 50m), time increment (0.005s, 0.01s, 0.02s), and turbulence modeling (k-ε, SST k-ω, RSM) in relation to the rupture rate of the inversion layer. The optimal combination of parameters is established as a 10m³ grid, a 0.01s time increment, and the Realizable k-ε model, achieving a relative error of less than 8%.Verification Using Multi-Source Data Initial field validation is conducted by integrating sounding data (temperature, humidity, pressure, wind speed) with PM2.5 measurements from the Urumqi Station at 08:00, ensuring a geopotential height error of less than 15m. Pollutant Verification Hourly data from the PM2.5 monitoring network operated by the Environmental Protection Bureau is evaluated, yielding a spatial correlation coefficient of R^2=0.76 ($p<0.01$) for the simulated concentrations.

4 Conclusion

This research investigates the process of destruction within the inversion layer by introducing disturbances at its base, aiming to establish a scientific foundation for artificial intervention in inversion phenomena and mitigating air pollution. The key findings are outlined as follows:

1. Disturbances at lower levels lead to a notable decrease in PM2.5 concentrations: Both the Fluent simulation conducted on a local scale and the ARPS simulation at a regional scale demonstrate a significant reduction in PM2.5 concentrations over time following the disturbances. After two hours, concentrations in local and regional contexts decrease by 30% and 25%, respectively. After three hours, these reductions grow to 50% and 45%, confirming that low-level disturbances facilitate the diffusion of pollutants by disrupting the inversion layer and enhancing atmospheric mixing.

2. Variations in concentration exhibit a positive correlation with turbulence intensity: Dynamic disturbances markedly increase the transportation capacity of the wind field and turbulence intensity due to an increase in inflow wind speeds (with an assumed increase of 30%-50% in the simulation). The reduction rate of PM2.5 concentrations shows a linear relationship with rising turbulent kinetic energy (TKE) (R^2=0.94). This suggests that employing artificial methods, such as mechanical devices designed to enhance wind turbulence, may effectively improve air quality during periods of inversion.

3. The dual-model joint simulation reveals purification mechanisms across multiple scales. The high-fidelity simulation conducted with Fluent effectively illustrates the process of "vortex breaking inversion - pollutant funnel-shaped diffusion" initiated by disturbances. Meanwhile, the meso-scale simulation performed using ARPS highlights how disturbances reshape urban airflow patterns, encompassing aspects such as cross-layer mixing induced by downward airflow and regional gradient diffusion. The integration of these two approaches provides cross-scale scientific insights into understanding pollution evolution during inversion events and the impact of intervention strategies.

4. Limitations of the research and avenues for future exploration: This study currently overlooks factors such as the effects of solar radiation, variations in terrain thermal characteristics (including valley winds), and the roughness of urban surfaces. Future efforts should focus on enhancing simulation accuracy by incorporating complex physical processes, including land surface models and radiation frameworks. Furthermore, in cities characterized by intricate topography like Urumqi, it will be essential to investigate the quantitative correlation between disturbance intensity, occurrence frequency, and reductions in pollutant levels to establish a foundation for developing a "precise disturbance" atmospheric pollution management strategy.

Funding

The writers would like to convey their appreciation to the Natural Science Foundation of the Xinjiang Uygur Autonomous Region (2024D01D33), and the Science and Technology Program of the Xinjiang Production and Construction Corps (2023AB036), and the China Desert Meteorology Science Research Foundation (Sqj2022018) for the assistance they provided.

References

1. Li Zhenjie, Ji Lili, He Qing., Characteristics of atmospheric mixing layer height and atmospheric stability in Urumqi region and their relationship with the atmospheric pollution. ARID LAND CE0CRAPHY42(3), 478–491(2019).
2. Liu Zilong, Dai Bin, Cui Zhuo yan., Concentration characteristics and potential source of atmospheric pollutants, A case study in Urumqi. ARDID ZONE RESEARCH38(2), 562-569(2021).
3. Brook R.D., Rajagopalan S., Pope C.A., Particulate matter air pollution and cardiovascular disease, An update to the scientific statement from the American Heart Association. Circulation121, 2331–2378 (2010).
4. Li Xia, Yang Jing, Ma Jun., Researches of weather pattern and boundary layer structure characteristics on serious air pollution days in Urumqi. Plateau Meteorology31(5),1414- 1423(2012).
5. Li Xia, Jia Jian., Research of the influence of the air flows on multiple scales on the trans port and diffusion mechanisms of urban air pollution over the complex terrains. Desert and Oasis Meteorology 10(6), 1-10(2016).
6. Zhao Keming, Li Xia, Lu Xinyu., Wintertime temporal- spatial distribution characteristics of air pollutants in the mountain gap town Urumqi. Arid Land Geography37(6), 1108- 1118(2014).
7. HE Yongqing, ZHAO Yucheng, FENG Shuqing., Temperature inversion in Xining city, Characteristics and correlation with air pollutant concentrations. Journal of Glaciology and Geocryology 36(3), 608–613(2014).
8. Xu Junli, Han Haidong, Wang Jian., Recharge sources and potential source areas of atmospheric PM2.5 in Xinjiang. Arid Zone Research40(6),874-884(2023).
9. Liu Zilong, Dai Bin, Cui Zhuoyan., Concentration characteristics and potential source of atmospheric pollutants, A case study in Urumqi. Arid Zone Research,38(2),562-569(2021).
10. LU R, R P TURCO., Air pollutant transport in a coastal environment. II: Three - dimensional simulations over Los Angeles basin. Atmospheric Environment36(6),1499–1518(2019)
11. ADANDOU, E.BOSSIOLIM. TOMBROU., The Importance of Mixing Height in Characterising Pollution Levels from Aerosol Optical Thickness Derived by Satellite. Water, Air, and Soil Pollution: Focus2, 17–28(2002).
12. Luo Zhao wei, XiaoYing chuan, Huang Wen., Feasibility study on weather modification to eliminate haze 6(12), 54-57(2020).
13. Gao Janqiu, Feng Yongji, Xiao Weisheng., Techniques and Methods of Artificial Mist Removal32(1), 32-35(2010).

14. Li Lei, Hu Fei, Cheng Xueling., An application of FLUENT in the atmospheric environment of urban blocks. Journal of the Graduate School of the Chinese Academy of Sciences21(4),476-480(2004).
15. Jiang Dehai, Jiang Weimei, Miao Shiguang., Numerical simulation of airflow and pollutant distribution in urban street canyons. Environmental Science Research19(3),7-12(2006).
16. Li B, Chen K, Yang J. Statistical analysis of the effect of wintertime air quality improvement using weather modification technology in Shihezi[J]. Acta Scientiae Circumstantiae,41(11): 4396-4405(2021).
17. Chang C H, R N Meroney., Numerica1 and physica1 mode1ing of b1uff body f1ow and dispersion in urban street canyons. Wind Engineering & Industria1 Aerodynamics,89,1325-1334 (2001).
18. Deng Yuanchang, Liu Sha, Yu Zhi., Analysis of the influence of roughness in CFD simulation of the actual terrain wind field. Acta Energiae Solaris Sinica31(12),1644-1649(2010).